

# Morphology and Texture of High-Density Polyethylene–Polystyrene Blends Deformed by Plane-Strain Compression

Z. BARTCZAK,\* N. P. KRASNIKOVA,<sup>†</sup> and A. GALESKI

Centre of Molecular and Macromolecular Studies, Polish Academy of Sciences, Sienkiewicza 112, 90–363 Łódź, Poland

## SYNOPSIS

The blends of high-density polyethylene (HDPE) with atactic polystyrene (PS) were deformed plastically by plane-strain compression in a channel die. The samples were deformed up to the true strain 1.8 (compression ratio 6) in three temperature regimes: below, near, and above the glass transition temperature of polystyrene component. The morphology and the texture of crystalline component in the deformed blend samples were investigated by means of scanning electron microscopy and wide angle X-ray diffraction (pole figures technique). It was found that the deformation process in the blend of immiscible HDPE and PS does not differ markedly from the deformation of the one-component system from the point of view of the deformation mechanisms involved. The crystalline textures of the blend samples are qualitatively the same as in the plain HDPE deformed under similar conditions. The active deformation mechanisms are the same in deformation of both the plain HDPE and HDPE/PS blend. The mechanism identified are crystallographic slips: (100)[001], (100)[010], and (010)[001] supported by the interlamellar slip. The presence of PS in blends modifies to some extent the deformation process and resulting orientation of the crystalline component of HDPE by modification of the stress distribution within HDPE matrix around PS inclusions. This influence is much stronger at low deformation temperatures, when PS is in a glassy state, than at temperatures above  $T_g$  of PS. © 1996 John Wiley & Sons, Inc.

## INTRODUCTION

The successful application of polymer blends with crystallizable components mostly depends on their high ability to plastic deformation upon action of excessive loads. Such polymer blends are generally applied as elements that bear loads. The plastic deformation behavior of the blends under high or excessive forces is then of special importance and interest. Usually, the studies of plastic deformation behavior include only the stress–strain relationship and investigation of changes of morphology of the blends on the level of the size of inclusions. The

energy absorption is also often considered. The behavior under impact conditions, when stresses quickly arise and the liquid like phase of the crystallizable component becomes glassy, were studied in greater details. Little was learned for slow dynamic and quasi-static loads when the amorphous phase is in the rubbery state.

One of the effects of plastic deformation is to impart preferred molecular orientation into crystalline and amorphous components. Although modern blends are capable of accommodating a high degree of plastic deformation, there are virtually no investigations that include the texture evolution in polymer blends due to large plastic deformation.

Frequently, the plastic deformation of homopolymers as well as polymer blends is accompanied by strong cavitation. It occurs mostly when tensile, bending, or shearing loads are applied. Significant

\* To whom correspondence should be addressed.

<sup>†</sup> On leave from Topchiev Institute of Petrochemical Synthesis, Russian Academy of Sciences, 117912-GSP Moscow V71, Russia.

Journal of Applied Polymer Science, Vol. 62, 167–179 (1996)

© 1996 John Wiley & Sons, Inc.

CCC 0021-8995/96/010167-13

internal cavitation of the type noted in tensile experiments, referred to as "micronecking" by Peterlin,<sup>1</sup> has been considered for a long time to be essential for large strain deformation of aggregates of chain-folded crystallites, where it was thought to remove kinematical constraints between lamellae and permit them to unravel. However, there are other modes of deformation with some constraints preventing internal cavitation. In plane-strain compression, by virtue of the large superimposed pressure component during deformation, there is no significant internal cavitation of the type observed in tensile experiments. It was shown<sup>2</sup> for homopolymers that when no internal cavitation is involved, the plastic deformation is crystallographic in nature while the amorphous component deforms in a manner to accommodate the rotation and slips of the crystalline phase. It is expected that the plastic deformation of polymer blends by methods that superimpose a large-pressure component during deformation will not produce intense cavitation, neither within the crystallizable component nor at polymer-polymer interfaces. The constraint of cavitation will expose the real crystallographic nature of plastic deformation in polymer blends. The cavitation is the reason that textured polymer blends are of little use for most applications. However, voidless highly textured polymer blends prepared by an appropriate deformation process may be of primary importance to material science.

The aim of this work is to turn attention to the crystallographic nature of plastic deformation imposed on a polymer blend and apply the concepts of crystallographic slips, interlamellar sliding, and rotation of lamellae carrying associated amorphous material. The presented, more rigorous, approach to plastic deformation of polymer blends containing a crystallizable component involves the studies of crystal plasticity and associated deformation of the amorphous phase. It is expected that in the case of immiscible polymers, containing up to 20 vol % of the dispersed component, the plastic deformation will be dominated by the matrix. On the microscopic level, however, local disturbances of stresses will appear, caused by the misfit of mechanical properties of the matrix and the dispersed material. As a result of the disturbances in the close vicinity of inclusions, other mechanisms than those in undisturbed regions will be activated, so the orientation of the material will not be as homogeneous as for the crystallizable polymer alone. It is also expected that the deformation of the system should depend very much on the glass transition temperatures  $T_g$  of the components.

## EXPERIMENTAL

The materials used in the present study were high-density polyethylene, HDPE (Lupolen 5261Z, BASF;  $M_w = 5 \times 10^5$ ,  $M_w/M_n = 13$ , Melt Flow Index (21.6 kg) 1.8 g/10 min, density 0.952 g/cm<sup>3</sup>) and atactic polystyrene, PS (Polistyren SC, Polish product;  $M_w = 3.48 \times 10^5$ ,  $M_n = 1.08 \times 10^5$ , Melt Flow Index (2.16 kg) 0.7 g/10 min, density 1.08 g/cm<sup>3</sup>).

Blends containing 0, 20, and 80 wt % of PS were blended by extrusion in a single-screw extruder (L/D = 20) at 200°C. In order to improve the dispersion of components, the extrusion process was repeated for each composition up to three times. The pellets of the obtained blends were compression molded at 180°C and 200 atm to form a 12 mm thick plaque. The mold was then cooled down to 114°C, held at this temperature for 1 h to allow polyethylene to crystallize at isothermal conditions, and, finally, quickly cooled to the room temperature with ice water. The time for isothermal crystallization was long enough to complete the spherulitic crystallization of all HDPE in the whole volume of the plaque. The isothermal regime of crystallization of the plaques was chosen in order to ensure a comparable supermolecular structure of the HDPE component in all samples prior to deformation experiments. From the molded plaques the outer skin layers (up to 1 mm from each side) were removed by machining to obtain the samples of the blends in the form of rectangular plates 50 × 60 mm and 10 mm thick. As revealed by X-ray measurements, the obtained core plates had a crystallinity of polyethylene near 70% and no traces of any crystallographic orientation anisotropy.

The machined plates of the blends were used for the deformation experiments. The plane-strain compression in a channel die (see Fig. 1) was chosen as the deformation method in this study. Channel die plane-strain compression is kinematically very similar to plane-strain tension. It results in a uniaxial flow of the polymer in plane-strain conditions. The advantages of applying such a mode of deformation is that the deformation is homogeneous in the whole range of the strain without global (as necking) or local instabilities, and avoids internal cavitation and related artifacts. Moreover, it is possible in this way to produce a relatively large sample of highly oriented material (approximate size 50 × 10 × 10 mm), which may be used for various further tests. The compression in the channel die was performed at three selected temperatures: 85, 95, or 100°C. The load to the plunger of the channel die

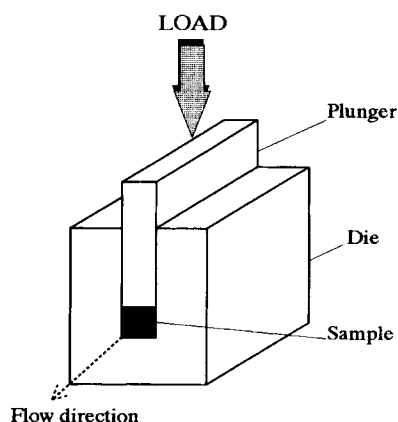


**Figure 1** Channel die device for a sample preparation by the plane-strain compression.

was applied using an Instron Testing Machine Model 1114T. The same crosshead speed of 1 mm/min was used in all experiments (the initial deformation rate,  $\dot{\epsilon}$ , was  $0.000277 \text{ s}^{-1}$ ). The compression was terminated near a compression ratio of 6 (reduction of the sample height from 60 to 10 mm). After compression, the sample was slowly cooled to room temperature without removing it from the die. The other details of the deformation procedure have been described elsewhere.<sup>2-4</sup>

The orientation of polyethylene crystalline phase in the deformed samples was studied by means of X-ray diffraction measurements. A WAXS system consisting of a pole figure device associated with a wide-angle goniometer (DRON 2, Russia) coupled to an X-ray generator operating at 30 kV and 30 mA ( $\text{CuK}_\alpha$  radiation, filtered electronically and by an Ni filter) was used in this study for X-ray measurements. The complete pole figures were obtained for projections of Euler angles of sample orientation with respect to an incident beam,  $\alpha$  (polar angle) from 0 to  $90^\circ$  and  $\beta$  (azimuthal angle) from 0 to  $360^\circ$ , both in  $10^\circ$  intervals. The specimens of the size  $10 \times 10 \text{ mm}$  and 1.5 mm thick were cut out from the oriented bars of blends perpendicularly to the loading direction. The following diffraction reflections from the orthorhombic crystal structure of polyethylene were analyzed: (200), (020), and (002) (diffraction angle,  $2\theta \approx 24, 36.4, \text{ and } 74.4^\circ$ , respectively). The construction of full pole figures required the connection of the X-ray data collected in the transmission and reflection modes. The connecting angle  $\alpha_c$  was  $40^\circ$  for the (200) and (020) reflections, while  $30^\circ$  for the (002) reflection. The slit system of the diffractometer was selected to measure the integral intensity of the appropriate diffraction peak. After the collection of data, the necessary corrections

for background scattering and sample absorption were calculated. An additional correction for the X-ray defocusing and other instrumental effects was performed using the data obtained at identical experimental conditions for a randomly oriented standard specimen of the HDPE. The specimen of HDPE of the same size and thermal history as the samples studied but having not deformed spherulitic morphology was used as a standard specimen. The pole figure plots were generated by the program POD, a part of the popLA package (Los Alamos National Laboratory, Los Alamos, NM).

The morphology of the samples was examined by scanning electron microscopy (SEM) in samples with appropriate surfaces exposed by cutting with a microtome (glass knife) and etching with toluene to remove the near-surface PS phase.

A DuPont TA-2000 differential scanning calorimeter (DSC) was used to study the melting behavior of the specimens. The heating rate was  $10^\circ\text{C}/\text{min}$ . For calculation of the overall crystallinity of polyethylene from DSC data, the heat of fusion of 100% crystalline polyethylene was taken as  $\Delta_f = 293 \text{ J/g}$ .<sup>5</sup>

The densities of the specimens were determined by means of a gradient column filled with a mixture of ethyl alcohol, water, and dissolved sodium chloride. The temperature of the column was maintained at  $23^\circ\text{C}$ .

## RESULTS AND DISCUSSION

Figure 2 presents plots of mechanical response of the blend samples subjected to plane-strain compression in a channel die at various temperatures. Figure 2(a) shows the stress-true strain curves of the compressed plain HDPE. It is seen that for HDPE deformed at  $85^\circ\text{C}$  the stress-strain plot represents a typical curve with initial elastic response followed by yielding, plastic flow, and strain-hardening processes. For higher compression temperatures, 95 and  $100^\circ\text{C}$ , the stress-strain curves are very similar in shape. The slope in the elastic region is practically the same for all temperatures. However, the yield stress decreases as temperature of deformation increases. Similarly, the stresses accompanying the plastic flow and strain hardening processes are lower when the deformation temperature increases. This shift towards lower stress is due to a decrease of the critical stress for the crystallographic slips controlling the plastic deformation

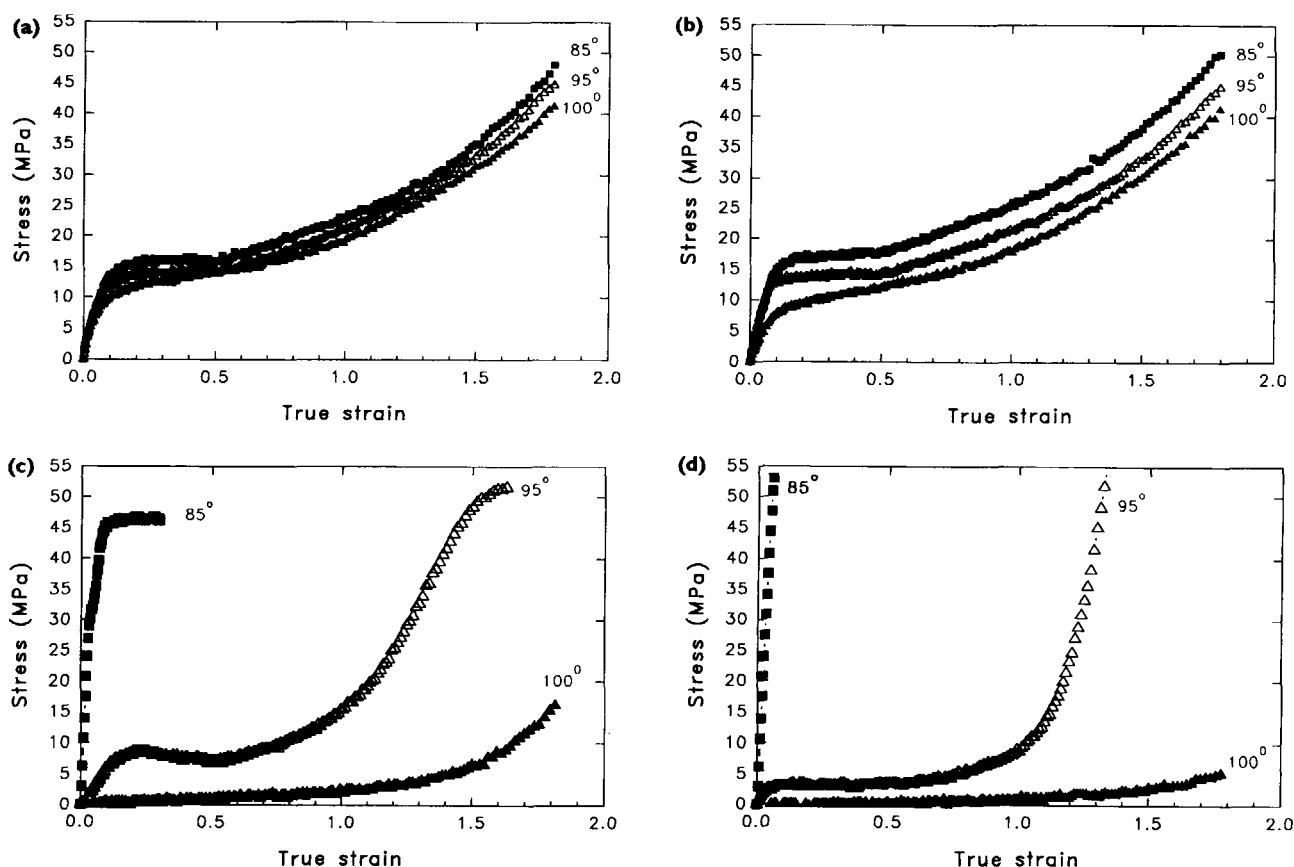


**Figure 2** The true stress-true strain curves of the plane-strain compression in a channel die: (a) plain HDPE; (b) 8 : 2 HDPE/PS blend; (c) 2 : 8 HDPE/PS blend; (d) plain PS. The temperature of deformation is indicated on each curve.

of HDPE, with an increase of deformation temperature.<sup>6</sup>

Figure 2(b) shows the stress-true strain plots for the 8 : 2 HDPE/PS blend. It is seen that the curves obtained for temperatures of compression 85, 95, and 100°C are similar in shape to those of the plain HDPE compressed at respective temperatures. A comparison of the curves presented in Figure 2(a) and (b) reveals that in the 8 : 2 blend deformed at 85°C the elastic modulus is a little higher and the curve in the range of plastic deformation is shifted towards higher stress in comparison to the plain HDPE deformed at the same temperature. At that temperature PS is in a glassy state ( $T_g$  of PS is 94°C, as determined by DSC) and its inclusions are considerably stiffer than the HDPE matrix, which leads to an increase of the stress level during the deformation process. When deformation temperature is set to 95°C both, plain the HDPE and 8 : 2 blend show nearly an identical mechanical response in the whole strain range. This temperature is within the range of glass transition of polystyrene; thus, the

PS particles have plastic resistance lower than they have in the glassy state. This resistance is comparable with the plastic resistance of the HDPE matrix, so that the mechanical behavior of the blend is very close to that of plain HDPE. At a deformation temperature of 100°C, which is above the  $T_g$  of polystyrene, the 8 : 2 blend has a lower elastic modulus compared to lower deformation temperatures as well as compared to the plain HDPE. Moreover, yielding and plastic flow occur at lower stress than in the plain HDPE deformed at 100°C. Such mechanical behavior reflects a rubberlike character of the PS minor component during deformation.

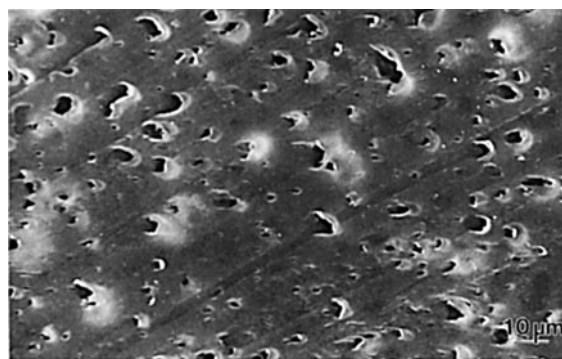
The mechanical behavior of the samples in which PS is a major component is completely different from that described above. Figure 2(c) shows the stress-strain curves of the 2 : 8 HDPE/PS blend, and Figure 2(d) those for the plain PS deformed at various temperatures. Plain PS deformed at 85°C shows brittle behavior and fractures at very low strain. In the case of the blend containing 80% of the PS, the stress-strain plot increases initially, as

for PS; however, at the level of stress of 30 MPa, a small shoulder is produced, which probably corresponds to the yield of the HDPE component. True yield of the blend is clearly seen at the level of 47 MPa. Following a short plastic flow the sample fractures in the channel along the planes tilted approximately 45° to the loading direction and eventually breaks.

When the deformation temperature is set in the range of the  $T_g$  of the PS (95°C), the deformation behavior changes dramatically: polystyrene, softening close to this temperature shows under compression yielding at the level of 4 MPa followed by long plastic flow up to the true strain of 0.8–0.9. Above that strain a region of very intensive strain hardening is observed, which may indicate an intense orientation of PS molecules. The 2 : 8 HDPE/PS blend deformed at that temperature shows similar behavior, although the yield and plastic flow occur at higher stress (ca. 8 MPa). Additionally, a significant depression of stress is observed during plastic flow. This is followed by a pronounced strain-hardening region. Such mechanical behavior of the blend is, no doubt, the effect of reinforcement of the PS matrix by the HDPE dispersed phase, which also participates in the strain accommodation.

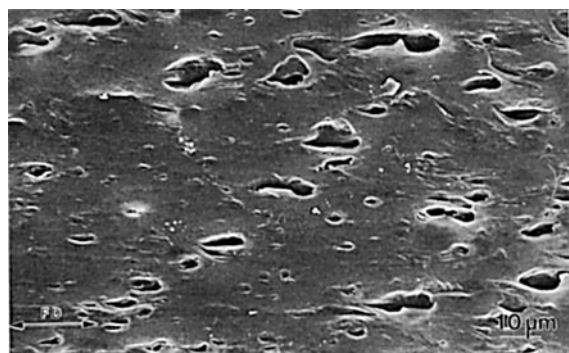
At temperatures above the  $T_g$  of the PS (100°C), the plastic flow of both the plain PS and the 2 : 8 HDPE/PS blend starts immediately after loading, with neither an initial elastic region nor yielding. Above the true strain of 1.0, a strain-hardening region can be observed in both samples. That strain hardening is much more pronounced and begins at a lower strain in the 2 : 8 blend than in the plain PS. The presence of strain hardening in the PS also indicates that at the high temperature some orientation of the PS chains is produced. The higher stress built up during the strain hardening of the 2 : 8 blend reflects the deformation and orientation of the HDPE dispersed phase in addition to flow-induced orientation of the PS matrix.

Figure 3 shows the scanning electron micrograph (SEM) of the undeformed 8 : 2 HDPE/PS blend. It is seen that HDPE forms a continuous matrix, whereas PS forms inclusions of the size of several micrometers dispersed in the matrix (only the sites previously occupied by PS inclusions instead of the inclusions are seen as the holes on the specimen surface because polystyrene was etched out with toluene). Figures 4–6 present the SEM micrographs of the same blend deformed to the true strain near 1.8 (compression ratio close to 6) at temperatures of 85°C (Fig. 4), 95°C (Fig. 5), and 100°C (Fig. 6). In each figure three views along flow direction, load-

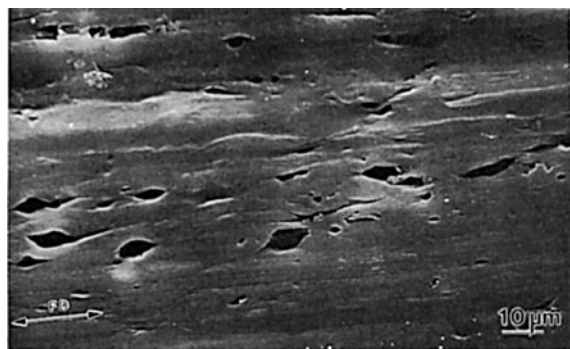


**Figure 3** Scanning electron micrograph of the 8 : 2 HDPE/PS undeformed blend.

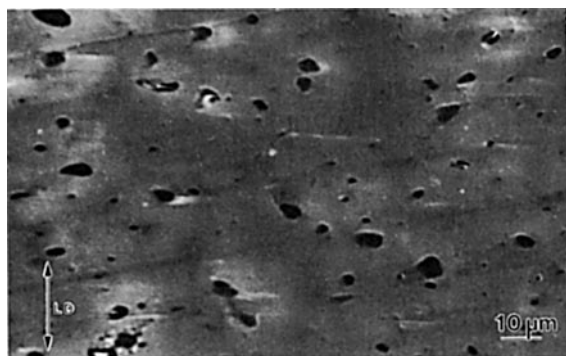
ing direction, and transverse direction are presented (FD, LD, and TD, respectively; see Fig. 1 for the reference). Figures 4–6 demonstrate that the PS inclusions undergo plastic deformation and orientation but the amount of the deformation strongly depends on the temperature of the deformation process. Compression performed at 85°C leads to a relatively small permanent deformation of PS inclusions (Fig. 4); the traces of inclusions visible on micrographs are slightly elongated in the flow direction, while the crosssection perpendicular to this direction shows nearly circular-shaped inclusion sites. The deformation of the inclusions at 85°C was much smaller than the overall sample deformation. PS is below its glass transition during the deformation process; thus, it is much harder than the embedding HDPE matrix. Hence, the strain could be accommodated almost entirely by the HDPE phase. It is also possible that some cavitation takes place on the interfaces in the direction of flow and the true deformation of the PS inclusion is even smaller than suggested by micrographs (note that we observed the vacancies in the HDPE matrix formed after dissolution of PS rather than the inclusion themselves; see also further discussion of the density). On the contrary, the deformation performed at 95 and 100°C, for instance, near and above the  $T_g$  of the PS, respectively induces much larger plastic deformation of the PS inclusions. At 95°C the PS is much more compliant than at 85°C, and its inclusions are deformed readily, pursuing to some extent the deformation of the matrix. Figure 5 shows that they substantially elongate along the flow direction while reducing their size along the loading direction. At a deformation temperature of 100°C polystyrene, being above its glass transition temperature, flows easily under the load. Thus, the PS inclusions in the 8 : 2 blend are seriously deformed, accommodating a very high strain. Figure 6 shows that the



(a)



(b)



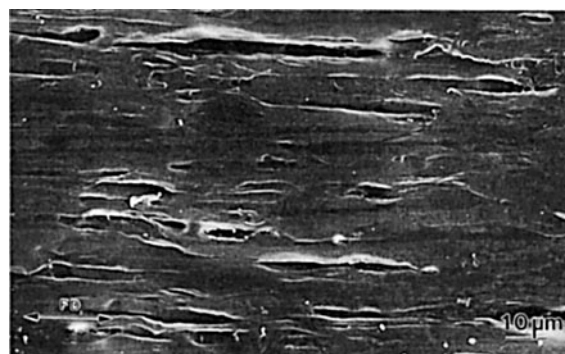
(c)

**Figure 4** Scanning electron micrograph of the 8 : 2 HDPE/PS blend deformed at 85°C; (a) view along the loading direction (FD-TD plane); (b) view along the transverse direction (LD-FD plane); (c) view along the flow direction (LD-TD plane).

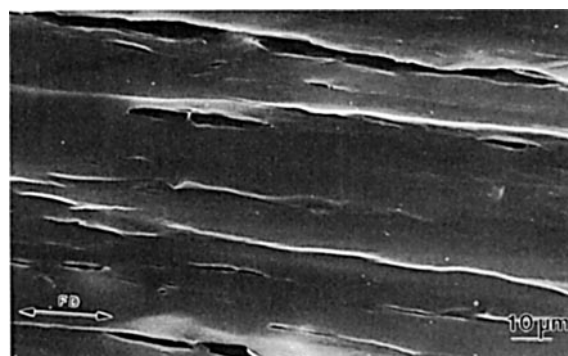
shape of the inclusions after deformation of the blend sample at 100°C is ribbonlike. The ribbons lie in the FD-TD plane and extend in the flow direction, FD. Such orientation reflects the plane-strain conditions of the deformation (constraints imposed on the sample in the transverse direction).

Figure 7 presents the bar chart of the density changes of the blend samples versus the deformation temperature. In the case of the plain HDPE, the plastic deformation in a channel die causes a small

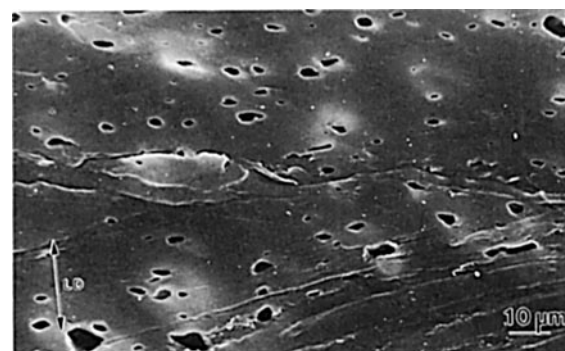
drop of the sample density. Similar drops were observed in the 8 : 2 and 2 : 8 HDPE/PS deformed blends, although the deformed 8 : 2 blend samples show an increase of the density with the increase of the deformation temperature. To interpret the observed variation of the density it is useful to compare the density data with the crystallinity data obtained from DSC measurements and presented in Figure 8 (in the absence of other effects the density is a linear function of the crystallinity degree). It is seen that



(a)

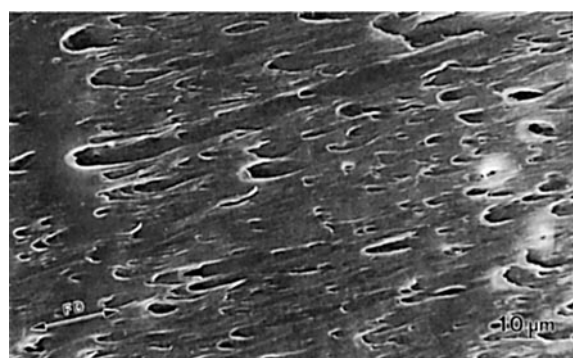


(b)

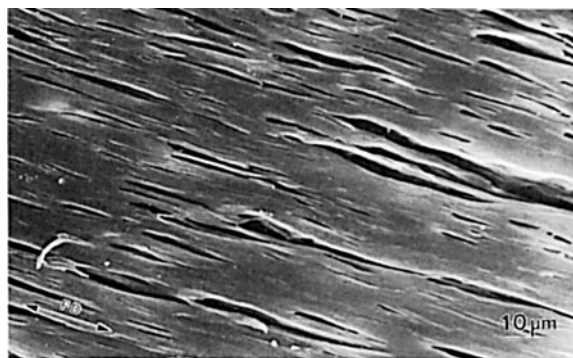


(c)

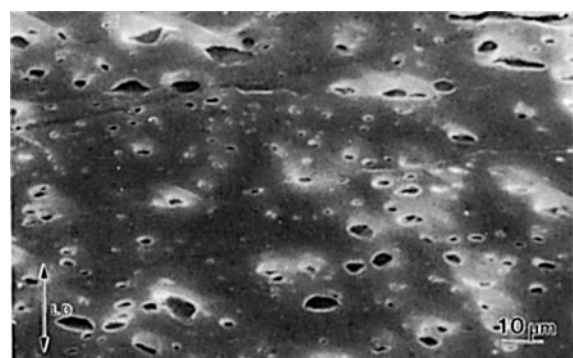
**Figure 5** Scanning electron micrograph of the 8 : 2 HDPE/PS blend deformed at 95°C; (a) view along the loading direction (FD-TD plane); (b) view along the transverse direction (LD-FD plane); (c) view along the flow direction (LD-TD plane).



(a)



(b)



(c)

**Figure 6** Scanning electron micrograph of the 8 : 2 HDPE/PS blend deformed at 100°C; (a) view along the loading direction (FD-TD plane); (b) view along the transverse direction (LD-FD plane); (c) view along the flow direction (LD-TD plane).

the changes of crystallinity of the plain HDPE follow those of density—a decrease of crystallinity due to deformation and its further decrease with increasing deformation temperature. This demonstrates that the density changes in the deformed HDPE result mostly from the reorganization of the crystalline phase including partial destruction during plastic deformation. The crystallinity of HDPE in the 8 : 2 blend changes in a similar fashion as in the plain HDPE samples, decreasing with an increase

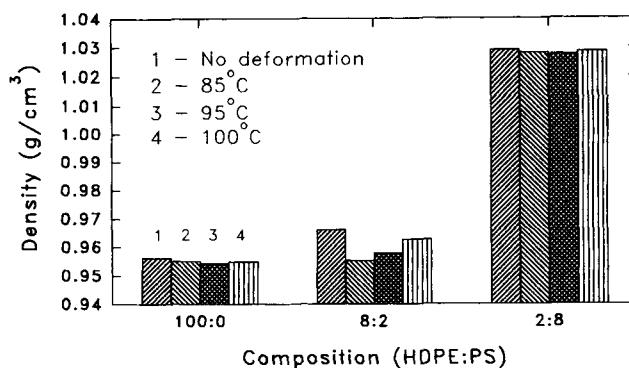


**Figure 7** The bar chart illustrating the dependence of the density on the blend composition and temperature of deformation. (1) Not deformed; (2) deformed at 85°C; (3) deformed at 95°C; (4) deformed at 100°C.

of the deformation temperature, which is contrary to the density variation. This may suggest the formation of voids on the PE-PS interfaces when the blend is deformed below the  $T_g$  of the PS. There is a substantial misfit of plastic resistances of components in the blend at such temperatures and their mutual adhesion is rather poor, which may promote cavitation at the interfaces, probably limited to the poles of the PS inclusions oriented along the flow direction (cavitation in other directions is constrained by compressive forces and external constraints). At higher temperatures rubbery PS is sufficiently soft to follow the deformation of the polyethylene matrix and the cavitation does not occur. In the 2 : 8 blend, again, the same trends as in plain HDPE were observed, for instance, density and crystallinity change in the same fashion, which suggest an absence of cavitation.

Figure 9 shows the melting behavior of HDPE in the deformed blends. It is seen that for every com-

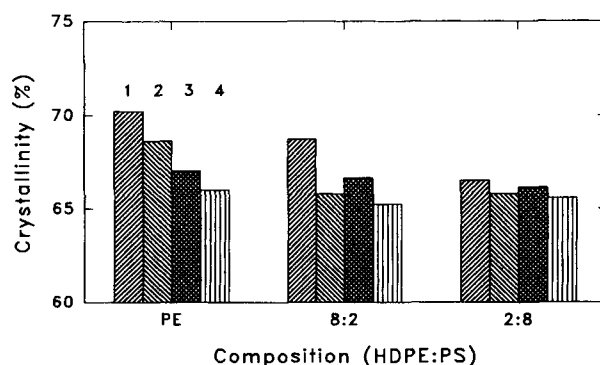


**Figure 8** The dependence of crystallinity on the blend composition and temperature of deformation. Samples: (1) not deformed; (2) deformed at 85°C; (3) deformed at 95°C; (4) deformed at 100°C.

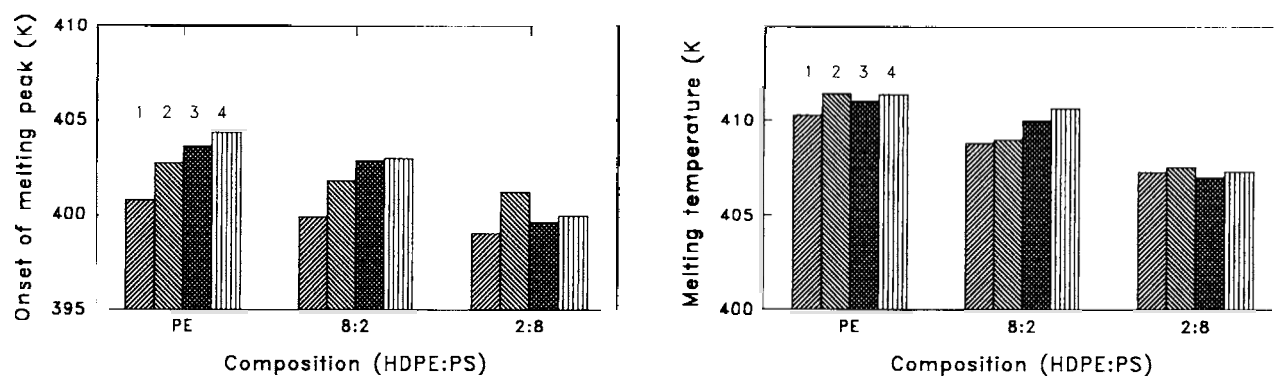


**Figure 9** Melting behavior of the blend samples in the dependence of composition and temperature of deformation: (a) temperature of the melting peak maximum; (b) temperature of the onset of melting peak. Samples: (1) not deformed; (2) deformed at 85°C; (3) deformed at 95°C; (4) deformed at 100°C.

position studied the onset of melting as well as the melting peak maximum were shifted towards higher temperatures. This, together with the above-mentioned decrease of crystallinity, indicates that the deformation induces a destruction of a fraction of the crystalline phase of the lowest thickness. Such conclusion is in accordance with the model of the evolution of the crystalline texture induced by plastic deformation,<sup>2</sup> according to which some limited destruction of the lamellae can happen during the plastic deformation in those parts of lamellae that have the smallest thickness.

Plain HDPE subjected to large plane-strain compression in a channel die develops a sharp single component texture with (100) planes of the orthorhombic crystals lying flat in the FD-TD plane while the *c* crystal axis contain chain axes oriented parallel

to the flow direction, FD.<sup>2,3</sup> A good illustration of such texture is a set of measured pole figures of the basic crystallographic planes: (200), (020), and (002); poles of these planes are equivalent to the crystallographic axes *a*, *b*, and *c*, respectively. Such a set of pole figures obtained from X-ray diffraction data for the plain HDPE compressed at 85°C to the true strain 1.8 is shown in Figure 10. In this figure, one can see the concentration of the poles of the (200) planes, for instance, *a* axis around the loading direction, the poles of (020) planes (*b* axis) around the transverse direction, and the poles of (002) planes (*c* axis, which is also the molecular axis) along the flow direction. This is a typical example of a well-developed single-component crystal texture of the (100)[001] type (classification according to the customs in metallurgy). The pole figures of the

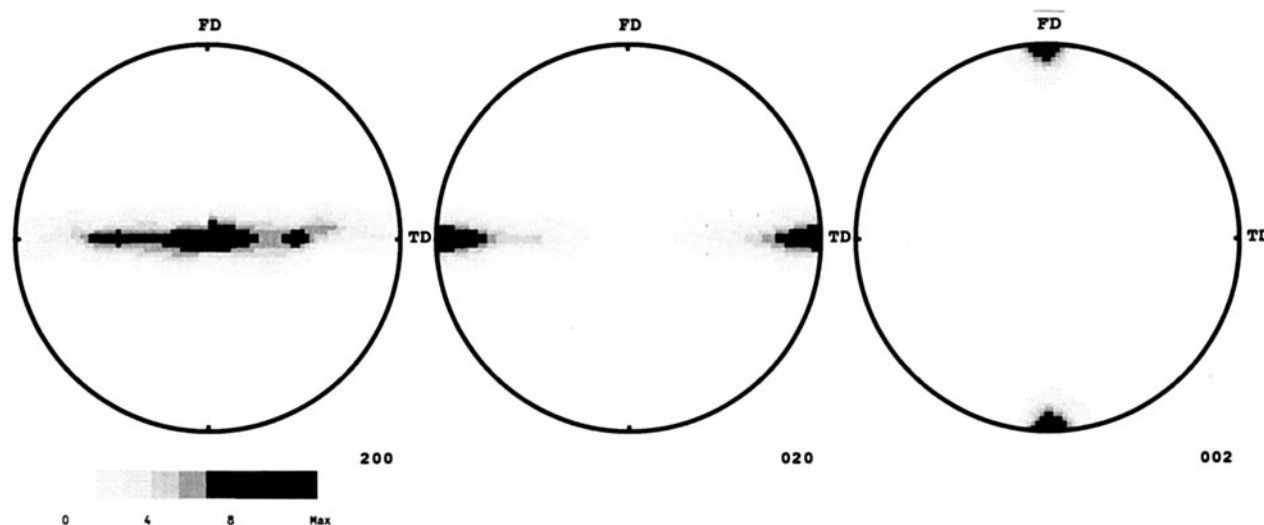


**Figure 10** The pole figures of (a) (200), (b) (020), and (c) (002) planes of the plain HDPE deformed by plane strain compression at 85°C.



respective planes of the HDPE samples compressed at 95 and 100°C (not shown here) look very similar to these presented in Figure 10, indicating that the change of the deformation temperature in the range studied does not influence the resultant texture, provided the strains are similar. Previous studies of the deformation behavior of HDPE under plane-strain compression<sup>2</sup> demonstrated that the final texture is a result of the activity of several crystallographical deformation mechanisms supported by the interlamellar shear of the amorphous interlamellar layers. The last mechanism is especially active at low and intermediate strains, and declines at a higher strain due to the saturation effect connected with the complete extension of tie molecules. The most active mechanism is the (100)[001] chain slip—the crystallographical slip acting in the (100) plane along the chain direction, [001]—with the critical resolved shear stress of 7.2 MPa. This mechanism is supported by two others slip systems—(100)[010] transverse slip (critical shear stress 12.2 MPa) and (010)[001] chain slip (critical shear stress 15.6 MPa).<sup>2,4</sup> Other deformation mechanisms known for polyethylene<sup>7,8</sup> have very limited activity.

Figures 11–13 show the pole figures of three basic planes of orthorhombic crystals of polyethylene—(200), (020) and (002) planes—obtained for the 8 : 2 HDPE/PS blend deformed at various temperatures, whereas Figures 14–16 present similar pole figures obtained for the 2 : 8 HDPE/PS blend. All the samples were compressed to the similar true strain close to 1.8, except the 2 : 8 HDPE/PS blend compressed at 85°C to a smaller strain due to pre-

mature breaking of the specimens. The X-ray diffraction intensity data used for construction of the pole figures were carefully corrected and normalized to the constant volume of the crystalline material in the sample to allow a direct comparison of the textures of the samples studied. From Figures 11–13 it is seen that in the 8 : 2 HDPE/PS blend the texture developed due to compression in a channel die generally shows the same features as in the deformed plain HDPE (compare with Fig. 10). However, in spite of the similar strain, the development of the texture strongly depends on the temperature at which the deformation process was carried out. The texture observed in the 8 : 2 blend deformed at 85°C is relatively weak and diffuse as compared to the plain HDPE, whereas that in the same blend deformed at 100°C is nearly as sharp as that of oriented plain HDPE. The results presented above indicate that during the deformation process of the 8 : 2 HDPE/PS blend the same mechanism is active, as in the case of the plain HDPE deformation. However, it is clear that the evolution of texture of polyethylene crystals in the blend was hindered when the deformation was carried out at 85°C, whereas no such effect was observed when the deformation was performed at 100°C. These differences can be attributed to different properties of the PS inclusions at these temperatures. At 85°C, the PS glassy inclusions are much stiffer than the HDPE matrix, thus causing a distinct modification of the stress distribution in their surroundings. It was demonstrated<sup>9</sup> that in the system consisting of a matrix and dispersed inclusions that are rigid compared to the matrix, and subjected to the uniaxial

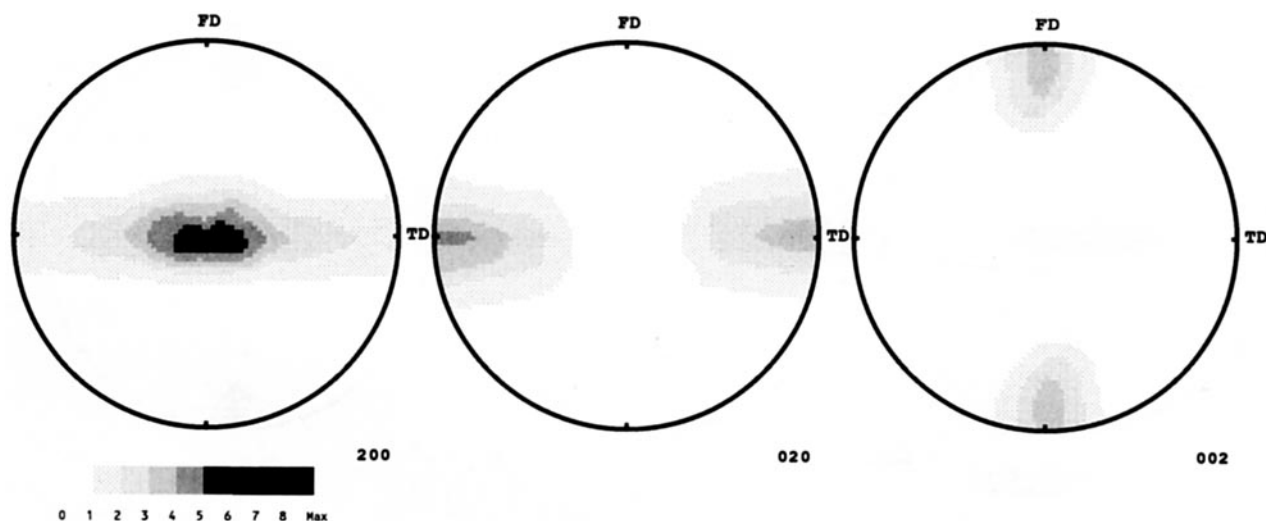


**Figure 11** The pole figures of (a) (200), (b) (020), and (c) (002) planes of the 8 : 2 HDPE/PS blend deformed by plane strain compression at 85°C.

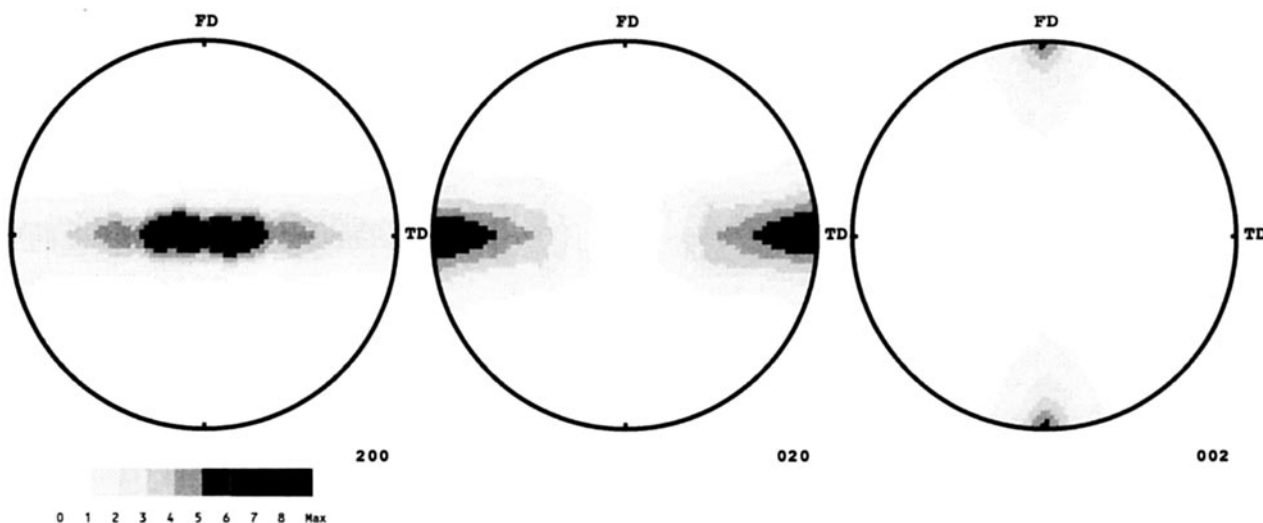


**Figure 12** The pole figures of (a) (200), (b) (020), and (c) (002) planes of the 8 : 2 HDPE/PS blend deformed by plane strain compression at 95°C.

deformation, the additional stresses are generated in the matrix around an inclusion: elongation stress in the direction of macroscopic elongation and compressive in perpendicular directions. These stresses are high enough to markedly alter the strain field of the matrix around inclusions; especially the strain accommodated by the matrix near the poles of the inclusion, which is higher than average, provided no cavitation at the interface occurs. In a similar way, during plane-strain compression in a channel die, the conditions for plastic deformation of the polyethylene matrix are different in the vicinity of the PS inclusion than away from it, where the stress distribution is not affected and is similar to that in

plain HDPE undergoing plastic deformation in the channel die. The consequence is that only a fraction of HDPE in the blend deforms at the stress conditions comparable to those in deformation of the plain HDPE, which leads to similar orientation of crystallites—(100)[001] crystal texture—whereas the remaining part of the HDPE matrix deforms in a different way due to locally modified stress. It must be emphasized that this difference in orientation is not the result of different deformation mechanisms involved, but results from a local variation of the conditions for the same mechanisms due to a variation in the stress distribution. That variation leads to a different activity of particular mechanisms or

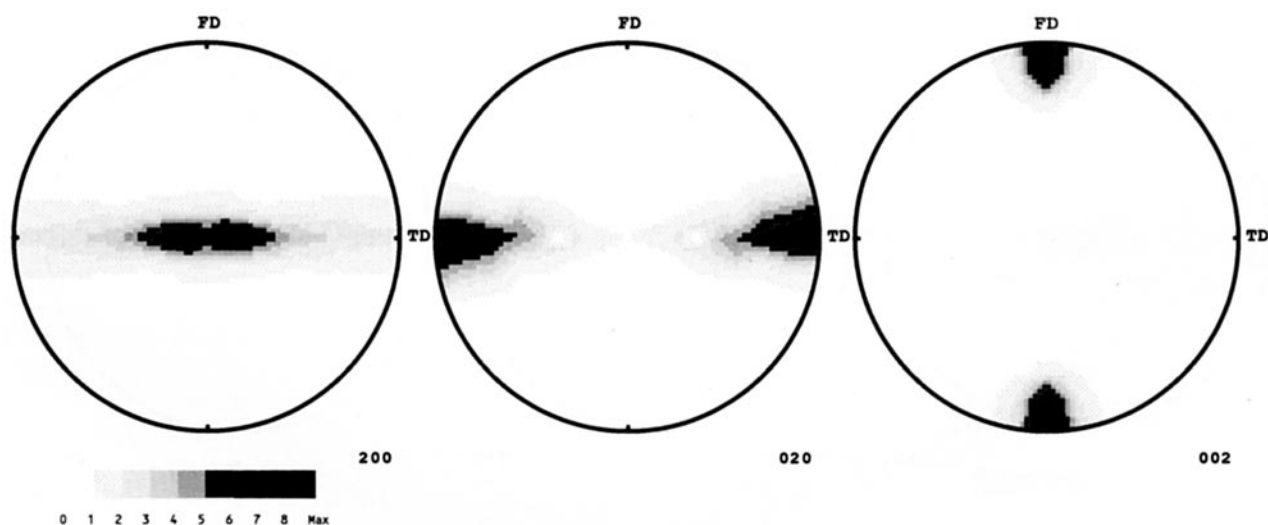


**Figure 13** The pole figures of (a) (200), (b) (020), and (c) (002) planes of the 8 : 2 HDPE/PS blend deformed by plane strain compression at 100°C.

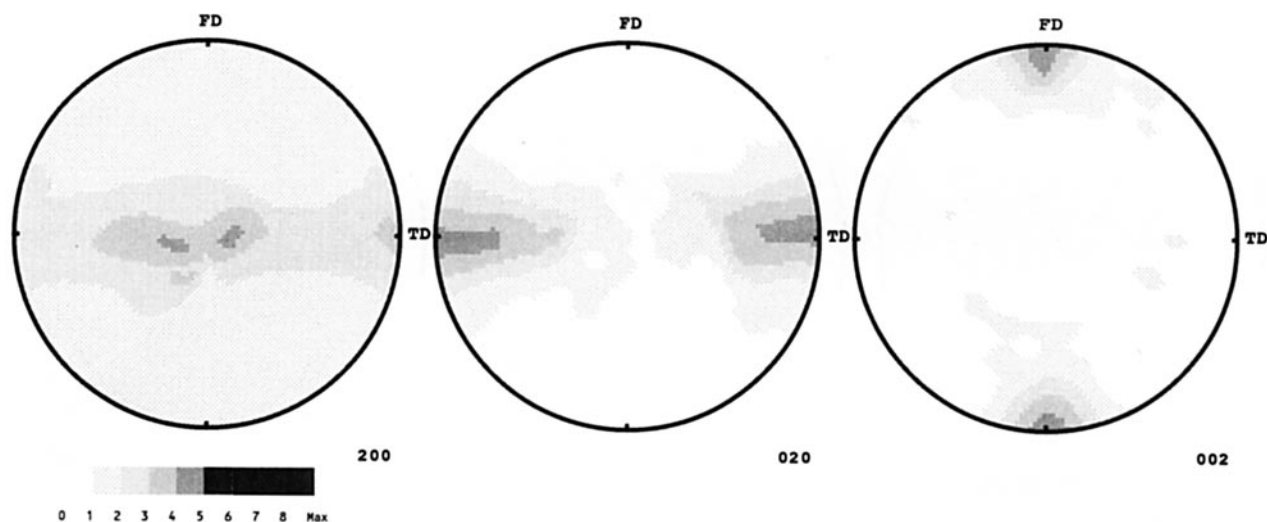


**Figure 14** The pole figures of (a) (200), (b) (020), and (c) (002) planes of the 2 : 8 HDPE/PS blend deformed by plane strain compression at 85°C.

even to the local modification of the sequence of the basic deformation steps (the deformation behavior of the matrix in the close vicinity of the inclusion is currently studied in detail). As a result, the overall texture of polyethylene crystals in the 8 : 2 HDPE/PS blend is still of the (100)[001] type, but it is much less developed than in the plain HDPE, in which all the crystallites deformed under the same stress conditions. In the case of the 8 : 2 HDPE/PS blend compressed at 100°C, the situation is different. At this temperature PS is above its glass transition temperature and shows a rubber-like behavior. The rubbery PS inclusions are much more compliant than the HDPE matrix, so the local stress

in the matrix in the inclusion vicinity is not so highly disturbed as it was in the case of glassy inclusions (deformation temperature 85°C). The presence of the inclusions causes only a minor modification of the stress distribution compared to the compressed plain HDPE. As a result, the final texture of polyethylene crystals in the plain HDPE and in the 8 : 2 blend do not markedly differ; both are sharp (100)[001] textures.

The textures of polyethylene crystals in the 2 : 8 HDPE/PS deformed blend samples are shown in Figures 14–16. The textures of these samples also give an impression of a (100)[001] crystal texture of plain HDPE, albeit they are even more diffused

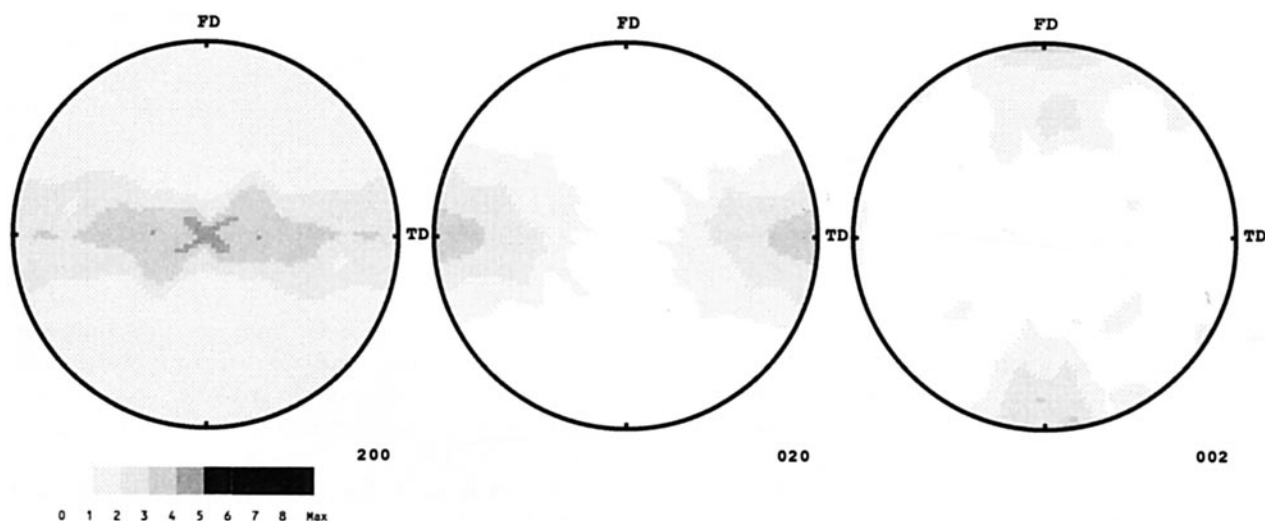


**Figure 15** The pole figures of (a) (200), (b) (020), and (c) (002) planes of the 2 : 8 HDPE/PS blend deformed by plane strain compression at 95°C.

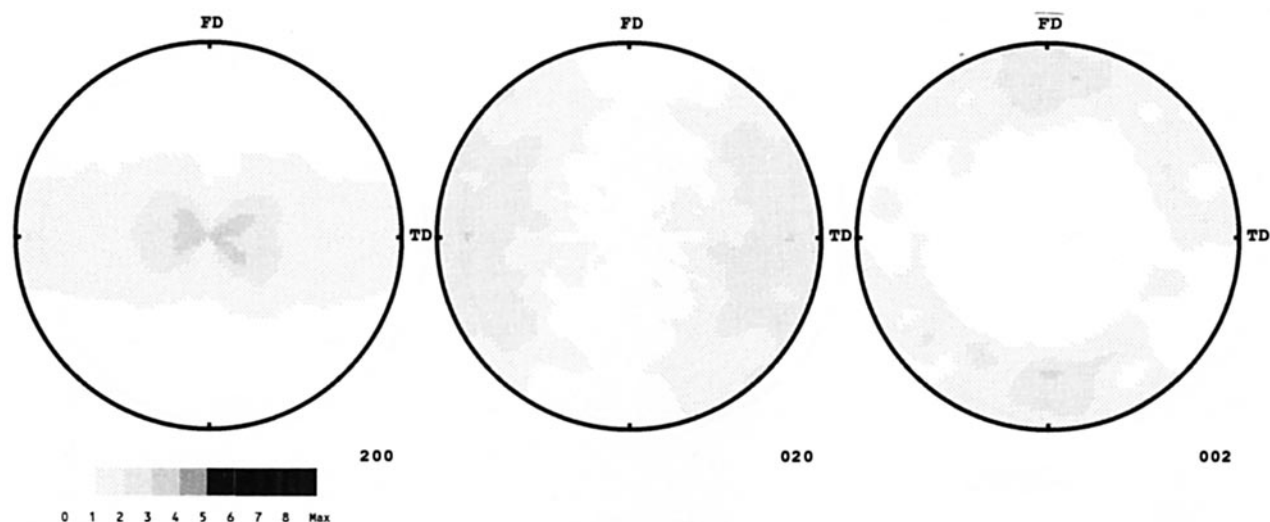


**Figure 16** The pole figures of (a) (200), (b) (020), and (c) (002) planes of the 2 : 8 HDPE/PS blend deformed by plane strain compression at 100°C.

than in the 8 : 2 HDPE/PS blend or the plain HDPE. Moreover, the higher the deformation temperature, the more diffused texture is observed, which is the opposite behavior to that of the previously reported composition. Note that the sample deformed at 85°C has the best developed texture in spite of the strain being lower than in the other samples of the 2 : 8 blend deformed at higher temperatures (deformation had to be interrupted at a lower strain due to premature fracture of the sample). This feature can be attributed to the morphology of the blend and again to the properties of the PS phase. Polystyrene constitutes in this blend a continuous phase, while polyethylene is dispersed in the form of highly elongated inclusions arranged in a quasicontinuous network, and the blend morphology resembles an interpenetrating polymer network. Such morphology is a result of the very high melt viscosity of the HDPE, compared to PS, and intensive and long mixing. Similar morphologies have been previously reported for blends of low-density polyethylene with polystyrene.<sup>10</sup> Loading the sample of this blend at a temperature below the  $T_g$  of the PS leads to high stress buildup in the sample and limited strain of the PS continuous phase. This high stress is transmitted through the glassy PS to the HDPE phase, where it causes a plastic deformation of both amorphous and crystalline components, although the overall strain accommodated by HDPE is also relatively low and comparable with the strain of the PS phase. However, the high stress level as well as its quick increase promotes the intense plastic deformation of the crystalline component at the expense of deformation of the amor-

phous component. As a result of such intense plastic deformation of crystallites a texture resembling the (100)[001] type texture develops in the 2 : 8 blend even faster than in the plain HDPE at a comparable strain. On the other hand, when the deformation temperature is in the range of or above the glass transition of PS (95 and 100°C, respectively) the PS phase is transformed to a rubbery state; thus, it can flow easy under a load. The stress generated on loading is substantially lower than that during the deformation at a lower temperature when it was in the glassy state. This stress transmitted to the HDPE inclusions is still enough to cause some plastic deformation of amorphous interlamellar layers by shear, but may be too low to induce an intense plastic deformation of the crystalline phase. In the case of deformation carried out at 100°C, the stress generated is too low to induce any plastic deformation of crystals up to the high overall strain where the strain hardening of the PS phase begins. The final orientation of crystals in this case results mostly from the rotations accompanying the interlamellar shear. In this way, the plastic deformation of the amorphous part of HDPE tends to dominate over the deformation of crystals in the deformation process with an increase of deformation temperature. Consequently, the texture of polyethylene crystals in the discussed 2 : 8 blend fades quickly when the deformation temperature increases above the  $T_g$  of the PS.

The textures of the 2 : 8 HDPE/PS blend have an additional feature observed neither in the blends in which HDPE is a major component nor in the plain HDPE. Examining the pole figures of the (200)

plane one can see that the intensity maxima outline the shape of a cross formed by two short lines intersecting in a center of the pole figure representing the loading direction, instead of a point or elliptical maximum typical for a one-component (100)[001] crystal texture. This shape is especially clear for the blend deformed at 95°C (cf. Fig. 15). In our opinion, this feature of HDPE orientation reflects the deformation of the amorphous PS matrix, which can tend to concentrate in intersecting shear bands at some deformation stage. We have observed formation of similar shear bands at intermediate strains in channel die compression of the HDPE and Nylon-6 samples.<sup>2,11</sup> The deformation of PS within the shear bands alters the local stress distribution, which should modify the deformation of the nearby HDPE phase. This, in turn, causes the modification of the orientation distribution of the HDPE crystalline component.

## CONCLUSIONS

On the basis of the results reported in this article several conclusions can be drawn. First, the plastic deformation of the semicrystalline polymer in the immiscible blend does not markedly differ from the deformation of the one-component system. The crystalline texture observed in the HDPE/PS blends deformed by plane-strain compression in a channel die are qualitatively the same as in the plain HDPE deformed under similar conditions. Second, the active deformation mechanisms are the same in plastic deformation of both the plain HDPE and the blend. These mechanisms, identified previously for HDPE<sup>2,4</sup> are the following crystallographic slips systems: (100)[001] chain slip as a dominating mechanism and (100)[010] transverse slip and (010)[001] chain slip as a secondary slip systems. The above crystallographic slips are supported by the interlamellar shear, the only mechanism active in the amorphous phase and not crystallographic in nature. Third, the obtained results suggest that the deformation process proceeding in the blend can be described by the same continuous sequence of the deformation mechanisms as for deformation of the semicrystalline polymer. Fourth, the presence of polystyrene in blends modifies to some extent the

resulting orientation of the crystalline phase of the HDPE. The modification strongly depends on the physical state of the PS in the course of the deformation process, which may be easily modified by changing the temperature of the deformation process. When the deformation of a HDPE-rich blend is carried out at a temperature below the glass transition temperature of the PS, the stiff inclusions of this polymer locally modify the stress distribution within the HDPE matrix and constitute an obstacle for the evolution of a uniform orientation. The orientation of polyethylene crystals in the vicinity of the PS inclusions is disturbed, which results in the final single-component crystal texture being less developed than in plain HDPE. When the deformation proceeds at temperatures above the  $T_g$  of the PS, its rubbery inclusions do not alter the stress distribution within the HDPE matrix as much. This results in the texture of the crystalline phase in the deformed blend being practically the same as in the deformed plain HDPE.

This research was supported by the State Comitee for Scientific Research (Poland) through project 7S20401306.

## REFERENCES

1. A. Peterlin, *Coll. Polym. Sci.*, **253**, 809 (1975).
2. A. Galeski, Z. Bartczak, R. E. Cohen, and A. S. Argon, *Macromolecules*, **25**, 5705 (1992).
3. H. H. Song, R. E. Cohen, and A. S. Argon, *Macromolecules*, **23**, 870 (1990).
4. Z. Bartczak, R. E. Cohen, and A. S. Argon, *Macromolecules*, **25**, 5036 (1992).
5. B. Wunderlich and C. M. Cormier, *J. Polym. Sci., Polym. Phys. Ed.*, **A-2**, 987 (1967).
6. Z. Bartczak, R. E. Cohen, and A. S. Argon, unpublished results.
7. P. B. Bowden and R. J. Young, *J. Mater. Sci.*, **9**, 2034 (1974).
8. L. Lin and A. S. Argon, *J. Mater. Sci.*, **29**, 294 (1994).
9. A. Pawlak and A. Galeski, *Coll. Polym. Sci.*, to appear.
10. M. Kozłowski, *J. Appl. Polym. Sci.*, **55**, 1375 (1995).
11. A. Galeski, A. S. Argon, and R. E. Cohen, *Macromolecules*, **24**, 3953 (1991).

Received March 18, 1996

Accepted April 24, 1996